

Simultaneous Optimization of Topology and Orientation of Anisotropic Material using Isoparametric Projection Method

Tsuyoshi Nomura¹, Ercan M. Dede², Tadayoshi Matsumori¹ and Atushi Kawamoto¹

¹Toyota Central R&D Labs., Inc. Aihchi, Japan, nomu2@mosk.tytlabs.co.jp

²Toyota Research Institute of North America, MI, USA,
eric.dede@tema.toyota.com

1. Abstract

New fiber reinforced composite fabrication technologies, such as tailored fiber placement or continuous fiber printing technology, enables realization of arbitrary orientation distribution of reinforcement fiber in a structure. Thus, building structures with optimal shape, topology and fiber orientation is now possible with aid of these technologies. In order to design such optimal structures, we propose a general topology optimization method, which is capable of simultaneous design of topology and orientation of anisotropic material, by introducing orientation design variables in addition to the density design variable. The proposed method supports not only discrete fiber orientation but also continuous fiber orientation design by using a Cartesian style orientation vector as the design variable combined with a projection method using isoparametric shape functions. The proposed method is less likely to be trapped at unwanted local optima when compared with classic continuous fiber angle optimizations, CFAOs, which directly uses orientation angle as the design variables; this is because vector representation offers more paths from one design solution to another, including an orientation vector with smaller norm, which represents weaker orientation. Another advantage of the proposed method is that it is compatible with filtering methods, especially design variable filtering, so that designers can control the complexity of the orientation angle distribution. The proposed method is built upon modern topology optimization technique, thus, it is versatile and flexible enough to solve multiload problems or even multiphysics problems.

2. Keywords: Topology optimization, Orientation design, Isoparametric projection, Tailored fiber placement, 3D printing

3. Introduction

Fiber orientation is the most important factor for demanding the mechanical properties of fiber reinforced composites such as carbon fiber reinforced plastics, CFRPs. In the past, fiber orientation design for such materials was rather limited. The composite is either unidirectional or woven fabric and the designers have to choose one option and can only determine the combination of given composites. These days, there are several new fabrication technologies that have become reality such as tailored fiber placement, TFP [1, 2], based on automated stitching machines, or continuous fiber printing systems [3] based on 3D printing technology. These technologies drastically expand the degree of freedom in orientation design of anisotropic composites, however, the design methodology to elicit maximum performance out of these technologies is not well established, yet. Topology optimization [4] looks to be the most forward thinking option to support this goal. Topology optimization was originally developed under consideration of anisotropy in material properties in the intermediate state by the homogenization design method with anisotropic microstructure, and there still has been enormous effort made for solving anisotropy topology optimization problems [5, 6, 7, 8]. In fact, solution of this anisotropic material layout problem has been demanded by the aerospace industry for a long time, and a large amount of effort has been made using a variety of numerical strategies [9, 10]. However, due to the difficulty in avoiding local optima [7, 11], a general optimization method has not been established yet, especially for the simultaneous optimization of topology and material orientation.

In this study, we propose a general topology optimization method, which is capable of simultaneous design of topology and orientation of anisotropic material, by introducing orientation design variables in addition to the density design variable by expanding the idea of design variable projection methods.

4. Formulation

In this paper, the formulation of the design variable is briefly summarized to focus the discussion. Readers are referred to the complete formulation as provided in a journal paper by the authors [12].

4.1. Topology design representation

Assume that a fixed design domain, D , is given, and inside of D , the following characteristic function is defined to indicate the object domain to be designed, Ω_d ;

$$\chi(\mathbf{x}) = \begin{cases} 0 & \text{for } \forall \mathbf{x} \in D \setminus \Omega_d, \\ 1 & \text{for } \forall \mathbf{x} \in \Omega_d. \end{cases} \quad (1)$$

Here, $\chi(\mathbf{x})$ is defined by an implicit function, ϕ , and Heaviside function such that

$$\chi(\mathbf{x}) = H(\phi(\mathbf{x})) = \begin{cases} 0 & \text{for } \forall \mathbf{x} \in D \setminus \Omega_d, \\ 1 & \text{for } \forall \mathbf{x} \in \Omega_d. \end{cases} \quad (2)$$

For regularization of the function space, a Helmholtz filter is used[13, 14],

$$-R_\phi^2 \nabla^2 \tilde{\phi} + \tilde{\phi} = \phi, \quad (3)$$

where R_ϕ is the filter radius and $\tilde{\phi}$ is a filtered field. The regularized Heaviside function is introduced to relax $\chi(\mathbf{x})$ to the material density field $\rho(\mathbf{x})$

$$\rho(\tilde{\phi}) = \tilde{H}(\tilde{\phi}), \quad (4)$$

where $\tilde{H}(\tilde{\phi})$ is a regularized Heaviside function.

The constitutive tensor, e.g. the stiffness tensor for a structural problem, is interpolated between void and solid state using ρ

$$\mathbf{C}_\rho = \mathbf{C}_v + \rho^p (\mathbf{C}_s - \mathbf{C}_v), \quad (5)$$

where \mathbf{C}_ρ , \mathbf{C}_v , \mathbf{C}_s are the interpolated tensor, void tensor, and solid material tensor, respectively, and p is the density penalty parameter. In the following discussion, \mathbf{C}_s is extended to anisotropic materials with a material physical parameter orientation design variable.

4.2. Orientation design representation with Isoparametric projection

For simplicity, this discussion is focused on a two-dimensional case, hereafter. A Cartesian representation is chosen for the design variable, and the orientation field in a given fixed design domain is declared as follows;

$$\vartheta(\mathbf{x}) = \begin{bmatrix} \xi(\mathbf{x}) \\ \zeta(\mathbf{x}) \end{bmatrix}, \quad (6)$$

where

$$|\vartheta(\mathbf{x})| \leq 1 \quad \text{for } \forall \mathbf{x} \in D. \quad (7)$$

Let the $v(\mathbf{x})$ be the precursor design vector field having natural coordinate values, ξ and η , as its elements

$$v(\mathbf{x}) = \begin{bmatrix} \xi(\mathbf{x}) \\ \eta(\mathbf{x}) \end{bmatrix}, \quad (8)$$

where

$$\xi \in [-1, 1] \quad \text{and} \quad \eta \in [-1, 1]. \quad (9)$$

We then define the orientation vector field as follows;

$$\vartheta(\mathbf{x}) = \mathbf{N}(v(\mathbf{x})) = \begin{bmatrix} N_x(\xi(\mathbf{x}), \eta(\mathbf{x})) \\ N_y(\xi(\mathbf{x}), \eta(\mathbf{x})) \end{bmatrix}, \quad (10)$$

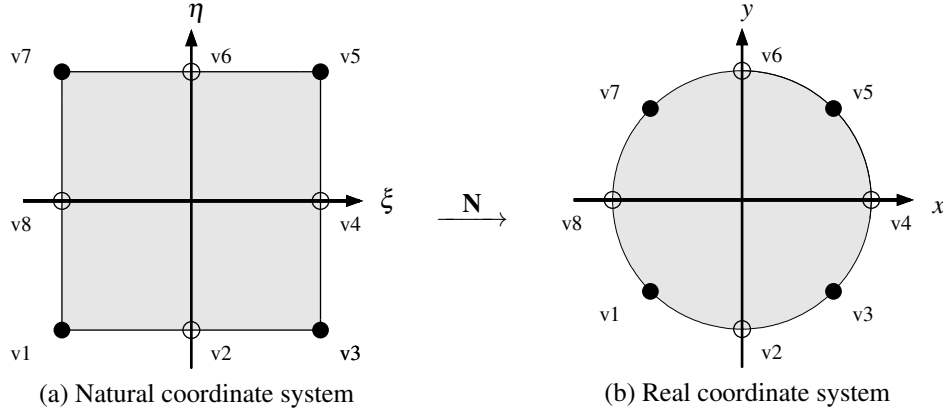


Figure 1: The eight node bi-quadratic serendipity element. Left: natural coordinates. Right: real coordinates.

where \mathbf{N} is an appropriate shape function whose boundary forms a unit circle. If the element is in the unit circle, then $\|\vartheta\| \leq 1$ is naturally fulfilled. There are various options in choosing an isoparametric shape function, \mathbf{N} , and the eight node bi-quadratic quadrilateral element [15, 16], namely the “serendipity” element, is used and defined as follows;

$$\begin{cases} N_x(\xi, \eta) = \sum_{i=1}^8 u_i N_i(\xi, \eta) \\ N_y(\xi, \eta) = \sum_{i=1}^8 v_i N_i(\xi, \eta), \end{cases} \quad (11)$$

where $\mathbf{v}_i = \{u_i, v_i\}^T$ is the coordinate of the i -th node in the real coordinate system, as shown in right side image of Figure 1. The function $N_i(\xi, \eta)$ is defined as follows;

$$\begin{cases} N_1(\xi, \eta) = - (1 - \xi)(1 - \eta)(1 + \xi + \eta) / 4 \\ N_2(\xi, \eta) = (1 - \xi)(1 - \eta)(1 + \xi) / 2 \\ N_3(\xi, \eta) = - (1 + \xi)(1 - \eta)(1 - \xi + \eta) / 4 \\ N_4(\xi, \eta) = (1 + \xi)(1 - \eta)(1 + \eta) / 2 \\ N_5(\xi, \eta) = - (1 + \xi)(1 + \eta)(1 - \xi - \eta) / 4 \\ N_6(\xi, \eta) = (1 - \xi)(1 + \eta)(1 + \xi) / 2 \\ N_7(\xi, \eta) = - (1 + \xi)(1 + \eta)(1 + \xi - \eta) / 4 \\ N_8(\xi, \eta) = (1 - \xi)(1 - \eta)(1 + \eta) / 2. \end{cases} \quad (12)$$

The relationship between ϑ and \mathbf{v} is analogous to the relationship between $\rho(\mathbf{x})$ and $\phi(\mathbf{x})$. Similarly, a Helmholtz filter is used to regularize \mathbf{v} , which resides in L^∞ space projected to H^1 space. However, this time, the regularized field is a vector field

$$\tilde{\mathbf{v}}(\mathbf{x}) = \begin{bmatrix} \tilde{\xi}(\mathbf{x}) \\ \tilde{\eta}(\mathbf{x}) \end{bmatrix}, \quad (13)$$

where \mathbf{v} has a box bound, but $\tilde{\mathbf{v}}$ does not have explicit bounds.

The regularization is enforced with the following equation

$$-\mathbf{R}_v \nabla^2 \begin{bmatrix} \tilde{\xi} \\ \tilde{\eta} \end{bmatrix} + \begin{bmatrix} \tilde{\xi} \\ \tilde{\eta} \end{bmatrix} = \begin{bmatrix} \xi \\ \eta \end{bmatrix}, \quad (14)$$

where $\mathbf{R}_v = R_v^2 \mathbf{I}$ and R_v is the filter radius for the vector field, and \mathbf{I} is the identity matrix. Then, unbounded $\tilde{\mathbf{v}}$ is projected into $-1 \leq \tilde{\xi} \leq 1$, $-1 \leq \tilde{\eta} \leq 1$ in a manner similar to the $\tilde{\phi}$ to ρ projection.

$$\bar{\mathbf{v}} = \begin{bmatrix} \tilde{\xi}(\mathbf{x}) \\ \tilde{\eta}(\mathbf{x}) \end{bmatrix} = \begin{bmatrix} 2\tilde{H}(\tilde{\xi}(\mathbf{x})-1) \\ 2\tilde{H}(\tilde{\eta}(\mathbf{x})-1) \end{bmatrix}. \quad (15)$$

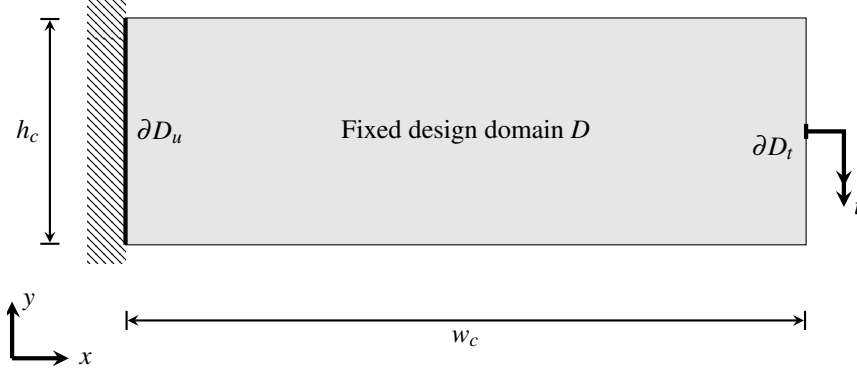


Figure 2: Geometry settings for the short cantilever problem.

In concert with equation (10), the regularized orientation field $\tilde{\vartheta}$ is obtained as follows;

$$\tilde{\vartheta}(\mathbf{x}) = \mathbf{N}(\bar{\mathbf{v}}(\mathbf{x})) = \begin{bmatrix} N_x(\bar{\xi}(\mathbf{x}), \bar{\eta}(\mathbf{x})) \\ N_y(\bar{\xi}(\mathbf{x}), \bar{\eta}(\mathbf{x})) \end{bmatrix} \quad \text{for } \forall \mathbf{x} \in D. \quad (16)$$

Finally, the constitutive tensor is transformed according to $\tilde{\vartheta}$

$$\mathbf{C}_a = \mathbf{C}_i + \hat{\mathbf{T}}^{-1}(\tilde{\vartheta}) \cdot (\mathbf{C}_u - \mathbf{C}_i) \cdot \hat{\mathbf{T}}'(\tilde{\vartheta}), \quad (17)$$

where \mathbf{C}_a is an interpolated tensor in terms of anisotropy, \mathbf{C}_u is a given unrotated anisotropic tensor, \mathbf{C}_i is an isotropic component subtracted from \mathbf{C}_u , and $\hat{\mathbf{T}}$ and $\hat{\mathbf{T}}'$ are transformations to rotate a tensor to a direction given by ϑ ; refer to the detailed description in a paper[12].

With this formulation, the following three states are continuously interpolated. When $\|\tilde{\vartheta}\| = 1$, this equation is equivalent to simple rotation of given \mathbf{C}_u , that is,

$$\mathbf{C}_a = \mathbf{T}^{-1}(\theta) \cdot \mathbf{C}_u \cdot \mathbf{T}'(\theta), \quad (18)$$

where $\theta = \angle \hat{\vartheta}$, and $\mathbf{T}(\theta)$ and $\mathbf{T}'(\theta)$ are rotation tensor for the stress tensor and strain tensor, respectively. This relationship holds owing to distributive property of tensor algebra and the isotropic nature of \mathbf{C}_i , that is, $\mathbf{C}_i = \mathbf{T}^{-1}(\theta) \cdot \mathbf{C}_i \cdot \mathbf{T}'(\theta)$. Therefore, if the design is converged to $\|\tilde{\vartheta}\| = 1$, it provides a purely orientation design result. When $0 < \|\tilde{\vartheta}\| < 1$, this allows the change of magnitude of anisotropy according to $\|\tilde{\vartheta}\|$, in addition to rotation according to $\angle \tilde{\vartheta}$. This provides a solution with orientation with various magnitude of anisotropy, that extends flexibility in change of design to help dynamic change during the optimization procedure to avoid local optima.

One major advantage is that this interpolation accepts the design variable $\mathbf{v} = \{0, 0\}^T$ that represents isotropic state. Therefore, the optimization procedure can be started from almost isotropic state to avoid influence of initial design orientation. Another important advantage of this approach is its bijective nature. This guarantees that design variables can be continuous if actual orientation distribution is continuous. Therefore, it works well with projection schemes without unphysical smear.

Substituting \mathbf{C}_s from (5) into the previous expression, the complete material interpolation function is finally defined as

$$\mathbf{C}(\rho, \vartheta) = \mathbf{C}_v + \rho^p (\mathbf{C}_i + \hat{\mathbf{T}}^{-1}(\tilde{\vartheta}) \cdot (\mathbf{C}_u - \mathbf{C}_i) \cdot \hat{\mathbf{T}}'(\tilde{\vartheta}) - \mathbf{C}_v). \quad (19)$$

5. Numerical example

A short cantilever benchmark problem where the left side is fixed and the middle of the right side is subjected to a surface loading is solved. The analysis geometry and boundary condition settings are as shown in Figure 2. The $w_c \times h_c$ rectangular domain is given as the analysis domain and the entire area is designated as a fixed design domain, D . The geometric parameters w_c and h_c are 3 and 1, respectively. The entire left side is fixed as ∂D_u , and ∂D_t is defined at the middle of the right side. The $-y$ directional surface load, t , on ∂D_t is set to unity and the length of ∂D_t is $h_c/10$. A square grid mesh with a side length of $d = 0.02$ is used in combination with Lagrange linear quadrilateral elements. The upper bound of volume fraction is set to 0.5.

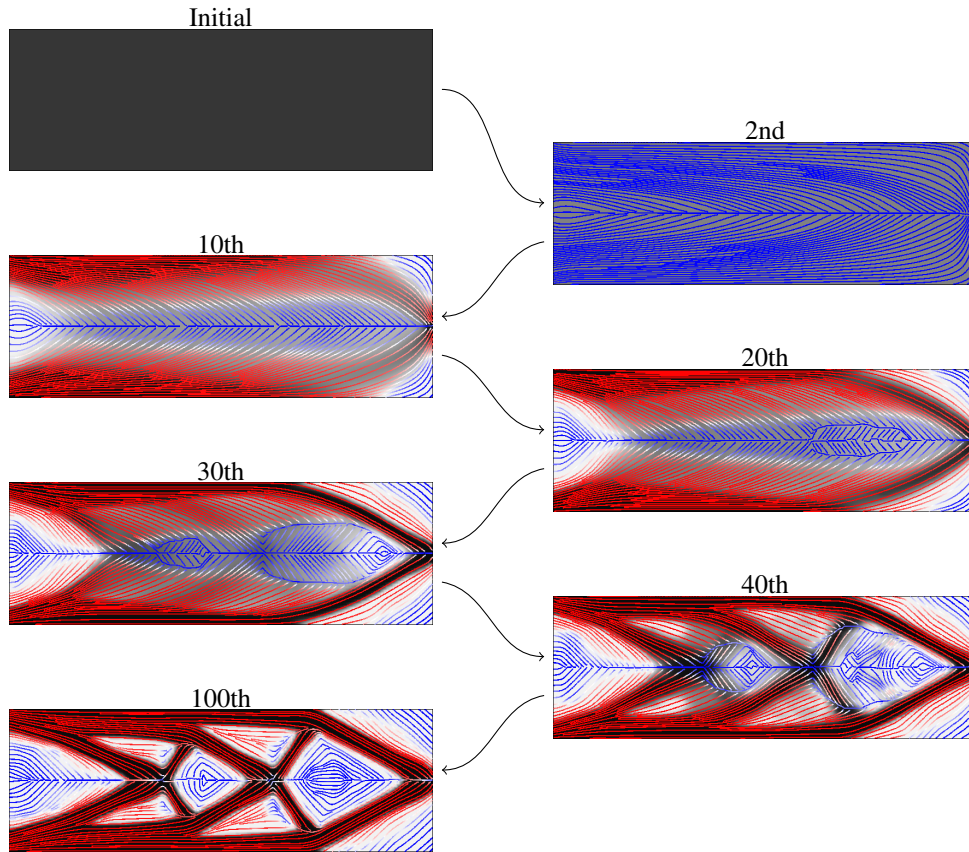


Figure 3: Optimization results for short cantilever problem with volume fraction 0.5. Configurations at various iteration steps are shown to describe evolution of the design. Gray scale image, stream line and color of the streamline indicate density, orientation direction and norm of orientation vector (blue: weak orientation, red: strong orientation), respectively

Figure 3 shows the obtained design solution. The figure shows eight configurations with various iteration steps to depict evolution of the topology and orientation distribution by the proposed method. The gray scale image on the background shows topology density, the stream line shows direction of orientation vector and the color of the stream line shows the norm of the orientation vector. Blue stream line shows that the orientation vector has small norm so that it has weak orientation, while red stream line shows that the orientation is strongly defined to a line direction. At the beginning, indicated as “initial” in the figure, the orientation vector design variable is uniform so that there is no stream line. At the second iteration, the stream lines appear and it is along with the principal stress direction of rectangular cantilever. At 10th step, non-uniform distribution of the density and orientation vector norm is recognized, but, it is still smooth except for the middle line and there is no large change in topology. At the 20th iteration, a site with different orientation direction is generated at the middle beam region with smallest density. At the 30th iteration, the number of discontinuous angle sites increases with and a hole is initiated at the tip of the cantilever. At the 40th iteration, the topology evolves to double cross configuration and the orientation distribution shows more complexity. Finally, at iteration 100, the topology becomes clear and the fiber reinforcement orientation angle is aligned with the small bars comprising the cantilever structure. Since it is single load problem, the obtained topology is almost identical to the one obtained by isotropic material optimization supporting empirical knowledge that the optimal orientation should coincide with the principal stress direction. Note that the orientation vector smoothly rotates as the topology progresses, and sometimes the change of the fiber orientation angle occurs prior to the topological change.

6. Conclusion

A topology optimization method which is capable of simultaneous design of topology and orientation vector using isoparametric projection method was reviewed. The method is based on density filter topology optimization

methods and an orientation vector is used for orientation representation along with a projection method using isoparametric shape functions. A benchmark example is provided and it shows a reasonable result.

7. Reference

- [1] P. Mattheij, K. Gliesche, and D. Feltin, "Tailored fiber placement-mechanical properties and applications," *Journal of Reinforced Plastics and Composites*, vol. 17, no. 9, pp. 774–786, 1998.
- [2] K. Uhlig, A. Spickenheuer, L. Bittrich, and G. Heinrich, "Development of a highly stressed bladed rotor made of a cfrp using the tailored fiber placement technology," *Mechanics of Composite Materials*, vol. 49, no. 2, pp. 201–210, 2013.
- [3] M. Namiki, M. Ueda, A. Todoroki, Y. Hirano, and R. Matsuzaki, "3D printing of continuous fiber reinforced plastic," in *Society for the Advancement of Material and Process Engineering 2014*, (Seattle), p. 6, SAMPE, jun 2014.
- [4] M. P. Bendsøe and N. Kikuchi, "Generating optimal topologies in structural design using a homogenization method," *Computer Methods In Applied Mechanics And Engineering*, vol. 71, pp. 197–224, 1988.
- [5] P. Pedersen, "Examples of density, orientation, and shape-optimal 2D-design for stiffness and/or strength with orthotropic materials," *Structural and Multidisciplinary Optimization*, vol. 26, no. 1-2, pp. 37–49, 2004.
- [6] K. Zhou and X. Li, "Topology optimization for minimum compliance under multiple loads based on continuous distribution of members," *Structural and Multidisciplinary Optimization*, vol. 37, no. 1, pp. 49–56, 2008.
- [7] J. Stegmann and E. Lund, "Discrete material optimization of general composite shell structures," *International Journal for Numerical Methods in Engineering*, vol. 62, no. 14, pp. 2009–2027, 2005.
- [8] T. Gao, W. Zhang, and P. Duysinx, "A bi-value coding parameterization scheme for the discrete optimal orientation design of the composite laminate," *International Journal for Numerical Methods in Engineering*, vol. 91, no. 1, pp. 98–114, 2012.
- [9] G. N. Vanderplaats, "Structural optimization-past, present, and future," *AIAA Journal*, vol. 20, pp. 992–1000, Jul 1982. doi: 10.2514/3.51158.
- [10] C. E. Harris, J. H. Starnes, and M. J. Shuart, "Design and manufacturing of aerospace composite structures, state-of-the-art assessment," *Journal of Aircraft*, vol. 39, pp. 545–560, Jul 2002. doi: 10.2514/2.2992.
- [11] R. Ansola, J. Canales, J. Tarrago, and J. Rasmussen, "On simultaneous shape and material layout optimization of shell structures," *Structural and Multidisciplinary Optimization*, vol. 24, no. 3, pp. 175–184, 2002.
- [12] T. Nomura, E. M. Dede, J. Lee, S. Yamasaki, T. Matsumori, A. Kawamoto, and N. Kikuchi, "General topology optimization method with continuous and discrete orientation design using isoparametric projection," *International Journal for Numerical Methods in Engineering*, 2014.
- [13] A. Kawamoto, T. Matsumori, S. Yamasaki, T. Nomura, T. Kondoh, and S. Nishiwaki, "Heaviside projection based topology optimization by a PDE-filtered scalar function," *Structural and Multidisciplinary Optimization*, vol. 44, no. 1, pp. 19–24, 2011.
- [14] B. S. Lazarov and O. Sigmund, "Filters in topology optimization based on helmholtz-type differential equations," *International Journal for Numerical Methods in Engineering*, vol. 86, no. 6, pp. 765–781, 2011.
- [15] I. Ergatoudis, B. Irons, and O. Zienkiewicz, "Curved, isoparametric, "quadrilateral" elements for finite element analysis," *International Journal of Solids and Structures*, vol. 4, no. 1, pp. 31 – 42, 1968.
- [16] D. Arnold and G. Awanou, "The serendipity family of finite elements," *Foundations of Computational Mathematics*, vol. 11, no. 3, pp. 337–344, 2011.